

# The influence of hopping on modulated photoconductivity

C Longeaud<sup>1</sup> and S Tobbeche<sup>2</sup>

<sup>1</sup> Laboratoire de Génie Electrique de Paris, (UMR 8507 CNRS), Supelec, Universités Paris VI et XI, 11 rue Joliot Curie, Plateau de Moulon, 91190 Gif sur Yvette, France

<sup>2</sup> Laboratory of Semiconductor and Metal Materials, Faculty of Science and Engineering, University Mohammed Khider, PO Box 145, Biskra 07000, Algeria

Received 25 July 2008, in final form 20 November 2008

Published 8 January 2009

Online at [stacks.iop.org/JPhysCM/21/045508](http://stacks.iop.org/JPhysCM/21/045508)

## Abstract

We have developed equations taking into account both multiple-trapping and hopping processes for describing transport phenomena in disordered semiconductors. These equations have been introduced into a numerical simulation to model the steady state dark conductivity and photoconductivity as well as the modulated photoconductivity. The influence of parameters such as the density of states and attempt-to-hop frequency on the results of these experiments has been investigated. Steady state and modulated photoconductivity experiments have been performed on a hydrogenated amorphous silicon film in the temperature range 18–300 K and the results have been compared with those from the numerical simulation. This comparison shows that the latter provides a suitable interpretation of the experimental behaviours observed in both experiments.

(Some figures in this article are in colour only in the electronic version)

## 1. Introduction

The modulated photocurrent (MPC) technique was proposed by Oheda [1] in the early 1980s and since then has undergone theoretical developments to enable it to be applied in investigations on the defects of highly resistive semiconductors and in particular hydrogenated amorphous silicon (a-Si:H) [2–4]. However, these approaches were based mostly on transport, trapping and recombination of carriers via a multiple-trapping (MT) process. In this MT model free carriers move by continuous trapping and release into and from localized states. The possibility of carrier hopping through the localized states was totally neglected although at low temperatures it may turn out to be the major transport contribution as suggested by experimental results [5–8]. Transport by hopping in a-Si:H has also undergone many theoretical developments, getting more and more sophisticated, until both hopping and multiple trapping had been taken into account [9–11]. However, these models were rather limited. For instance, only the conduction band tail states were assumed to be concerned in the hopping process. Besides, these models aimed to describe steady state photoconductivity when lots of experiments developed to probe defect states are based on transient photocurrent or modulated photocurrent

measurements. Recently, Marshall [12] has proposed another approach to the hopping process and it was shown that this approach could be applied to transient photocurrents [13, 14].

In this paper we have developed calculations based on the work of Marshall, introducing the gap state occupancy in the hopping probability to try to model both steady state and modulated photoconductivity. These calculations are presented in section 2. A numerical calculation was performed including these equations and we present in section 3 its application to the modelling of steady state dark conductivity and photoconductivity. In particular we show how the gap state occupation functions, calculated taking account only of the MT process, are modified when the hopping process is taken into account. In section 4, the numerical simulation is used to show the influence of the hopping process on the MPC data and how the density of states (DOS) reconstructed from the data is altered by hopping. Finally, in section 5, we present the results of steady state photoconductivity and MPC experiments that we have performed on an a-Si:H film in the range 18–300 K and compare the experimental results with the simulated ones. The calculation that we have developed seems to account properly for the experimental results for both the steady state and modulated photoconductivity.

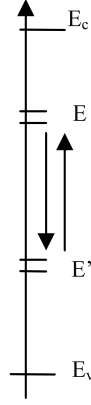


**Figure 1.** Scheme of transitions between two energy levels.

## 2. Theoretical development

To take into account the transport by the hopping process we have used the ideas developed by Marshall [12] for the analytical procedure for modelling of hopping and used by other authors to study transient photocurrent [13, 14], but we have tried to take the state occupancy into account. To simplify the presentation and mathematical treatment we have only considered states of one type in the band gap, defined by their capture coefficients for holes and electrons, as well as a single attempt-to-hop frequency. Nevertheless, these calculations could be extended easily to the case where localized states of several types are present in the band gap.

If we consider two levels in the gap at energies  $E$  and  $E'$ , of widths  $dE$  and  $dE'$  respectively and with  $E' < E$  (see figure 1), exchanging electrons we can write at any time  $t$

$$\frac{\partial g(E)f(E) dE}{\partial t} = -C_{nE'}g(E)f(E) dEg(E') \times (1 - f(E')) dE' + e_{nE',E}g(E')f(E') dE' \quad (1)$$

where  $g(E)$  is the density of states at energy  $E$ ,  $f(E)$  the occupation function,  $C_{nE'}$  the capture coefficient for the level at  $E'$ , and  $e_{nE',E}$  the rate of emission from the level at  $E'$  towards the level at  $E$ . Under dark equilibrium conditions equation (1) transforms into

$$0 = -C_{nE'}g(E)\frac{f(E)}{1 - f(E)}(1 - f(E))(1 - f(E')) dE + e_{nE',E}f(E'), \quad (2)$$

which, taking account of the expression for  $f$  under dark conditions, leads to

$$e_{nE',E} = C_{nE'}g(E)(1 - f(E)) dE \exp\left(-\frac{E - E'}{k_bT}\right), \quad (3)$$

in which  $k_b$  is the Boltzmann constant and  $T$  the temperature. Of course it is only simple detailed balance but one can see that the state occupancy is taken into account via the term  $(1 - f(E))$ . For instance if states between  $E$  and  $E + dE$  are full, electrons from states in between  $E'$  and  $E' + dE'$  cannot hop upward onto level  $E$ .

In the case of a distribution of states, we have taken an expression for  $C_{nE'}$  identical to that proposed by Marshall [12]:

$$C_{nE'} = \frac{\nu_0}{\int_{E_v}^E g(E') dE'} \exp\left(-\frac{2r_E}{R_0}\right) \quad (4)$$

where the mean intersite spacing is given by  $r_E = (\int_{E_v}^E g(E') dE')^{-1/3}$ ,  $E_v$  being the energy level of the top of the valence band,  $R_0$  the decay length of the wavefunction, and  $\nu_0$  the attempt-to-escape frequency for the hopping or attempt-to-hop frequency. In equation (4) for continuity in the notation we have kept the notation  $C_{nE'}$  coming from equation (2) but the reader may note that  $C_{nE'}$  does not depend on  $E'$  alone any longer, now depending on integrals over all the energies  $E'$  lower than  $E$ . We have defined the transition rates for hopping down from states at energy  $E$  into the underlying distribution, including isoenergetic hops, and the reverse, upward hops, via

$$P_{E,E'} = \frac{\nu_0}{\int_{E_v}^E g(E') dE'} \exp\left(-\frac{2r_E}{R_0}\right) g(E')(1 - f(E')) dE' = \Gamma_{E,E'}g(E')(1 - f(E')) dE', \quad (5)$$

$$P_{E',E} = \frac{\nu_0}{\int_{E_v}^E g(E') dE'} \exp\left(-\frac{2r_E}{R_0}\right) \exp\left(-\frac{E - E'}{k_bT}\right) g(E) \times (1 - f(E)) dE = \Gamma_{E',E}g(E)(1 - f(E)) dE,$$

respectively, for  $E' \leq E$ . The reader may note that the form of  $\Gamma_{E,E'}$ , as implicitly defined by equations (5), depends on the sign of  $E - E'$ . For instance, in the case where  $E \leq E'$  the  $E$  and  $E'$  have to be swapped in equations (5).

The rate equation for the occupancy of states between  $E$  and  $E + dE$  is identical to the one proposed by Marshall [12] but the main difference is that the state occupancy is taken into account in the hopping probabilities,

$$\frac{\partial f(E)}{\partial t} = (1 - f(E)) \int_{E_v}^{E_c} \Gamma_{E',E}g(E')f(E') dE' - f(E) \int_{E_v}^{E_c} \Gamma_{E,E'}g(E')(1 - f(E')) dE', \quad (6)$$

$E_c$  being the energy level at the bottom of the conduction band. This equation can be added to the rate equation for state occupancy via the multiple-trapping (MT) model and the whole system of continuity equations becomes

$$\frac{\partial n}{\partial t} = G - C_n n \int_{E_v}^{E_c} g(E)(1 - f(E)) dE + \int_{E_v}^{E_c} e_n(E)g(E)f(E) dE$$

$$\frac{\partial f(E)}{\partial t} = C_n n(1 - f(E)) - e_n(E)f(E) + e_p(E) \times (1 - f(E)) - C_p p f(E) + (1 - f(E)) \int_{E_v}^{E_c} \Gamma_{E',E}g(E')f(E') dE' - f(E) \int_{E_v}^{E_c} \Gamma_{E,E'}g(E')(1 - f(E')) dE'$$

$$\begin{aligned} \frac{\partial p}{\partial t} = & G - C_p p \int_{E_v}^{E_c} g(E) f(E) dE \\ & + \int_{E_v}^{E_c} e_p(E) g(E) (1 - f(E)) dE, \end{aligned} \quad (7)$$

assuming that a single species of states is concerned, i.e. the same capture coefficients for electrons and holes  $C_n$  and  $C_p$  respectively, these coefficients being assumed independent of the energy position. In this system,  $G$  is the rate of generation of carriers,  $n$  and  $p$  the free electron and hole concentrations respectively,  $e_n(E)$  and  $e_p(E)$  the rates of emission of electrons and holes from the localized states toward the conduction and valence band respectively.

This system can be solved in the steady state by defining a fine ladder of energy levels, each of width  $\Delta E$ , either by means of a Newton–Raphson technique directly applicable to steady state equilibrium or by means of an Euler implicit technique for which the time has to be taken long enough to ensure that the system has reached the steady state equilibrium. The matrices to be considered are full and thus taking hopping into account is a little bit more complicated than simple MT approaches, but routines are now available that give a reasonable time of calculation [15]. The advantage of the Euler implicit technique would be that one can also treat the problem of transient currents. In the calculations presented here we have used a Newton–Raphson technique to investigate steady state behaviours. The number of energy levels in the band gap was taken equal to 300. Below this number, the results of the simulation were dependent on the number of levels, especially at low temperature. Above this number we did not observe an evolution of the results with decreasing  $\Delta E$ .

The conductivity will be the sum of the conductivity via extended states and conductivity by hopping:

$$\begin{aligned} \sigma = & q\mu_n n + q\mu_p p + \frac{q^2}{6kT} \int_{E_v}^{E_c} g(E) f(E) \int_{E_v}^{E_c} \Gamma_{E,E'} g(E') \\ & \times [1 - f(E')] r_{E'}^2 dE' dE, \end{aligned} \quad (8)$$

an expression in which  $\mu_n$  and  $\mu_p$  are the electron and hole extended state mobilities respectively and  $q$  the absolute value of the electron charge. The reader may note that equation (8) uses hopping diffusivity and the Einstein equation which are only valid under low field conditions, where the field does not alter the probabilities of upward hopping.

Before revealing the treatment of the modulated photocurrent we would like to come back to the definition of the hopping coefficient  $C_{nE'}$ . Indeed, the reader may wonder whether it would not have been more appropriate to introduce a weighting factor in the denominator of  $C_{nE'}$  taking account of the state occupancy, that is  $\int_{E_v}^E g(E')(1 - f(E')) dE'$ , as well as in the definition of  $r_E$ . However, in that case, in addition to the fact that the state occupancy would be taken into account twice (once in the coefficient and once in the balance equation), we would have had to introduce equations to take account of the hopping of holes emitted from the valence band. Under dark conditions, the Fermi level could be taken as a limit between hopping of electrons above it and

hopping of holes below it, but under illumination the problem is much more complicated since some states in the middle of the gap, the recombination states, are expected to be only partly filled. Besides, one may consider that holes hopping up are just electrons hopping down with the same probability. The movement of holes one way being considered as the movement of electrons the other way, we think that considering only one type of particle (the electron) in the hopping process implies that the weighting factor at the denominator of  $C_{nE'}$ , as well as the integral in the definition of  $r_E$ , must take into account all the gap states, occupied or not, below the energy  $E$  to give a proper description of the complete hopping process.

To treat the case of the modulated photocurrent, all the quantities  $Q$  involved in equations (7) can be written as  $Q = Q_{dc} + Q_{ac} \exp(-j\omega t)$ ,  $\omega$  being the angular frequency, and  $j$  the complex number such that  $j^2 = -1$ . The amplitude of the alternating contribution,  $Q_{ac}$ , being considered as a small perturbation of  $Q_{dc}$ , equations (7) can be rewritten, neglecting the terms in  $\exp(-2j\omega t)$ , as

$$\begin{aligned} j\omega n_{ac} = & G_{ac} - C_n n_{ac} \int_{E_v}^{E_c} g(E) (1 - f_{dc}(E)) dE \\ & + C_n n_{dc} \int_{E_v}^{E_c} g(E) f_{ac}(E) dE \\ & + \int_{E_v}^{E_c} e_n(E) g(E) f_{ac}(E) dE \\ f_{ac}(E) \left( j\omega + \frac{1}{\tau(E)} \right) = & (1 - f_{dc}(E)) \left[ \int_{E_v}^{E_c} \Gamma_{E',E} g(E') f_{ac}(E') dE' + C_n n_{ac} \right] \\ & - f_{dc}(E) \left[ - \int_{E_v}^{E_c} \Gamma_{E,E'} g(E') f_{ac}(E') dE' + C_p p_{ac} \right] \end{aligned} \quad (9)$$

$$\begin{aligned} j\omega p_{ac} = & G_{ac} - C_p p_{ac} \int_{E_v}^{E_c} g(E) f_{dc}(E) dE \\ & - C_p p_{dc} \int_{E_v}^{E_c} g(E) f_{ac}(E) dE \\ & - \int_{E_v}^{E_c} e_p(E) g(E) f_{ac}(E) dE, \end{aligned}$$

where

$$\begin{aligned} \frac{1}{\tau(E)} = & C_n n_{dc} + e_n(E) + e_p(E) + C_p p_{dc} \\ & + \int_{E_v}^{E_c} \Gamma_{E',E} g(E') f_{dc}(E') dE' \\ & + \int_{E_v}^{E_c} \Gamma_{E,E'} g(E') (1 - f_{dc}(E')) dE'. \end{aligned} \quad (10)$$

The dc contribution has been cancelled in equations (9) because under steady state equilibrium these terms eliminate naturally. To go further, the alternating quantities are written as a sum of a real part and an imaginary one except for the generation rate. For instance,  $n_{ac}$  is written as  $n_{ac} = n_r + jn_i$ .

In this way equations (9) give rise to the following system of equations:

$$\begin{aligned}
 & -C_n n_r \int_{E_v}^{E_c} g(E)(1 - f_{dc}(E)) dE \\
 & + \int_{E_v}^{E_c} (C_n n_{dc} + e_n(E))g(E)f_r(E) dE + \omega n_i \\
 & = -G_{ac} \\
 C_n n_r (1 - f_{dc}(E)) + \int_{E_v}^{E_c} g(E')f_r(E')[(1 - f_{dc}(E)) \\
 & \times \Gamma_{E',E} + f_{dc}(E)\Gamma_{E,E'}] dE' - \frac{f_r(E)}{\tau(E)} + f_i(E)\omega \\
 & - C_p p_r f_{dc}(E) = 0 \\
 & - C_p p_r \int_{E_v}^{E_c} g(E)f_{dc}(E) dE \\
 & - \int_{E_v}^{E_c} (C_p p_{dc} + e_p(E))g(E)f_r(E) dE + \omega p_i \\
 & = -G_{ac} \\
 & -C_n n_i \int_{E_v}^{E_c} g(E)(1 - f_{dc}(E)) dE \\
 & + \int_{E_v}^{E_c} (C_n n_{dc} + e_n(E))g(E)f_i(E) dE - \omega n_r = 0 \\
 C_n n_i (1 - f_{dc}(E)) + \int_{E_v}^{E_c} g(E')f_i(E')[(1 - f_{dc}(E)) \\
 & \times \Gamma_{E',E} + f_{dc}(E)\Gamma_{E,E'}] dE' - \frac{f_i(E)}{\tau(E)} \\
 & - f_r(E)\omega - C_p p_i f_{dc}(E) = 0 \\
 & -C_p p_i \int_{E_v}^{E_c} g(E)f_{dc}(E) dE \\
 & - \int_{E_v}^{E_c} (C_p p_{dc} + e_p(E))g(E)f_i(E) dE - \omega p_r = 0.
 \end{aligned} \tag{11}$$

There is no particular mathematical difficulty concerning the resolution of this system except the huge size of the matrix to be considered. Indeed, this system can be solved numerically by defining a fine ladder of energy levels within the gap of the semiconductor considered. If the gap is divided into  $N$  energy levels, the number of variables to handle will be equal to  $2N + 4$ , two variables for  $n_{ac}$  ( $n_i$  and  $n_r$ ), two variables for  $p_{ac}$  ( $p_i$  and  $p_r$ ) and  $2N$  variables for  $f_{ac}$  ( $N$  for  $f_r$  and  $N$  for  $f_i$ ).

The photoconductivity can be calculated according to equation (8). A tedious but quite straightforward calculation, following the same lines as above, leads to

$$\begin{aligned}
 \sigma_r = q \left[ \mu_n n_r + \mu_p p_r + \frac{q}{6k_b T} \right. \\
 \times \int_{E_v}^{E_c} \left( f_r(E) \int_{E_v}^{E_c} \Gamma_{E,E'} g(E')(1 - f_{dc}(E')) r_{E'}^2 dE' \right. \\
 \left. \left. - f_{dc}(E) \int_{E_v}^{E_c} \Gamma_{E,E'} g(E') f_r(E') r_{E'}^2 dE' \right) g(E) dE \right]
 \end{aligned}$$

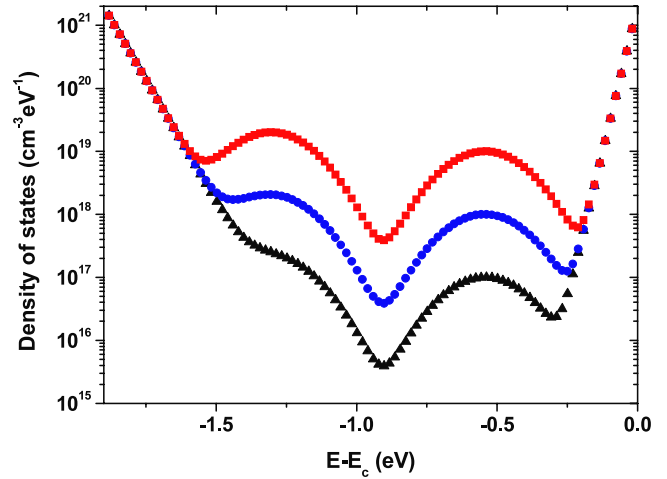


**Figure 2.** Typical densities of states introduced in the simulation to study the influence of hopping on the steady state and modulated photoconductivity.

$$\begin{aligned}
 \sigma_i = q \left[ \mu_n n_i + \mu_p p_i + \frac{q}{6k_b T} \right. \\
 \times \int_{E_v}^{E_c} \left( f_i(E) \int_{E_v}^{E_c} \Gamma_{E,E'} g(E')(1 - f_{dc}(E')) r_{E'}^2 dE' \right. \\
 \left. \left. - f_{dc}(E) \int_{E_v}^{E_c} \Gamma_{E,E'} g(E') f_i(E') r_{E'}^2 dE' \right) g(E) dE \right]
 \end{aligned} \tag{12}$$

for the real and imaginary parts of the conductivity, respectively.

The complete numerical simulation of the modulated photocurrent is achieved first by taking only the dc component of the flux into account to determine the gap state occupancy, and then, the state dc occupancy is assumed to be ‘frozen in’ during the calculation of the ac component of the current since the ac excitation is only a small perturbation of the dc one.

### 3. Steady state conductivity and photoconductivity

To illustrate this simple model we have introduced in the simulation densities of states (DOS) typical of hydrogenated amorphous silicon (a-Si:H) of different qualities. These DOS are displayed in figure 2.

The band gap was fixed at 1.75 eV. The characteristic temperatures of the conduction and valence band tails were chosen equal to  $T_c = 250$  K and  $T_v = 600$  K respectively, with a density of states at each band edge equal to  $2 \times 10^{21} \text{ cm}^{-3} \text{ eV}^{-1}$ . The equivalent densities of states at the conduction and valence band edges,  $N_c$  and  $N_v$  respectively, were taken equal to  $k_b T \times 2 \times 10^{21} \text{ cm}^{-3}$ , which gives  $N_c = N_v = 5 \times 10^{19} \text{ cm}^{-3}$  at 300 K. The deep states were made of two Gaussian distributions fixed at 0.5 and 1.2 eV below  $E_c$  with a standard deviation of 0.12 eV. The maxima of these distributions were equal to  $10^{17} \text{ cm}^{-3} \text{ eV}^{-1}$  (at 0.5 eV) and  $2 \times 10^{17} \text{ cm}^{-3} \text{ eV}^{-1}$  (at 1.2 eV) for the lowest density (full triangles) and were increased to  $10^{18} \text{ cm}^{-3} \text{ eV}^{-1}$  and  $2 \times 10^{18} \text{ cm}^{-3} \text{ eV}^{-1}$  (full circles) to reach  $10^{19} \text{ cm}^{-3} \text{ eV}^{-1}$

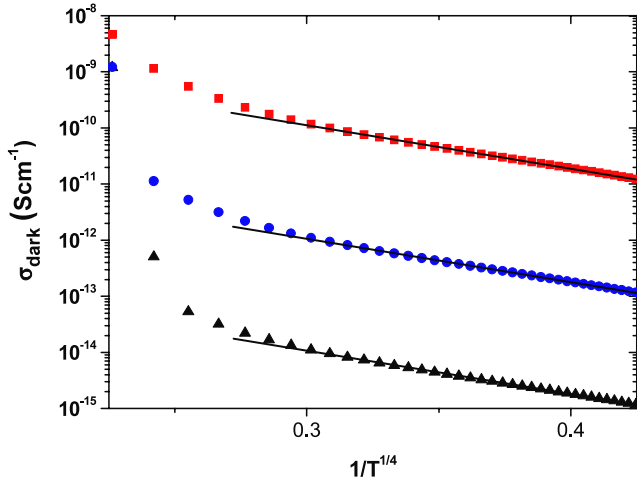


**Figure 3.** Dark conductivity versus  $1/T^{1/4}$  for the three densities of states of figure 2 (same symbols). The straight lines are guides for the eye.

and  $2 \times 10^{19} \text{ cm}^{-3} \text{ eV}^{-1}$  (full squares) respectively. Electrical neutrality sets the dark Fermi level slightly above mid-gap at 0.835 eV below  $E_c$ . The capture coefficients were taken identical for all the states:  $C_n = 10^{-8} \text{ cm}^3 \text{ s}^{-1}$  and  $C_p = 10^{-9} \text{ cm}^3 \text{ s}^{-1}$ . The extended state mobilities of electrons and holes were fixed at  $\mu_n = 10 \text{ cm}^2 \text{ V}^{-1} \text{ s}^{-1}$  and  $\mu_p = 0.3 \text{ cm}^2 \text{ V}^{-1} \text{ s}^{-1}$ . The decay length of the wavefunction  $R_0$  and the attempt-to-hop frequency  $\nu_0$  were fixed at  $5 \times 10^{-8} \text{ cm}$  and  $7 \times 10^{12} \text{ s}^{-1}$  respectively. These parameters were chosen because they correspond to the ‘usual’ values found in the literature for a-Si:H. Most of these parameters come from various experiments or from some recent studies on this material (see for instance [16] and references therein). We want to stress that our intention is not to use the ‘exact’ values in this paper but rather good orders of magnitude to illustrate our findings taking a-Si:H as an example.

In figure 3 we display the dark conductivity variations versus  $T^{-1/4}$  calculated using the simulation for the three different densities of figure 2. At low temperature the dark conductivity follows a law in  $\exp(-A/T^{1/4})$  predicted by Mott [17] when transport occurs predominantly by hopping around the dark Fermi level. Although this law in  $\exp(-A/T^{1/4})$  is at present a matter of controversy [18], it is clear that the low temperature conductivity is mediated by the hopping terms. It can also be seen that the higher the DOS around the Fermi level, the higher the hopping conductivity.

Since the simulation is reproducing the expected behaviours for steady state dark equilibrium, calculations were performed with the same parameters to study the photoconductivity. A generation rate of  $G = 10^{17} \text{ cm}^{-3} \text{ s}^{-1}$  was assumed and calculations were performed for the three DOS presented in figure 2. These calculations were done assuming that multiple trapping was involved alone in the transport of carriers or assuming that transport takes place by multiple trapping and hopping. Results are displayed in figure 4.

When MT is supposed to be the single process of transport (MT alone) the photoconductivity decreases with

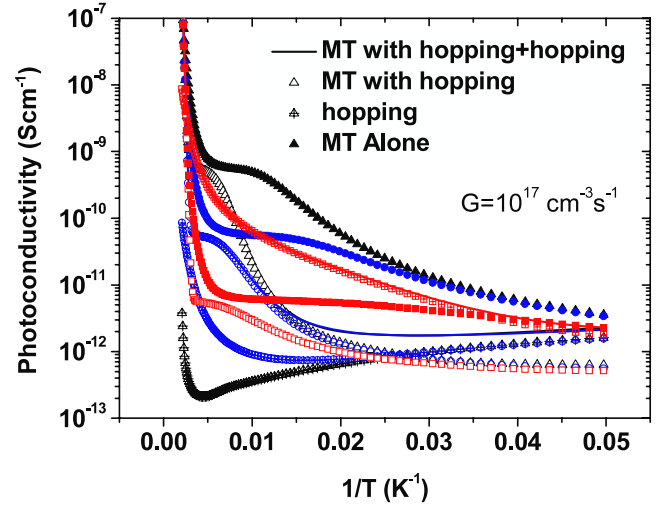


**Figure 4.** Photoconductivity calculated taking account of the multiple-trapping process alone (full symbols) or of both the MT and hopping processes for the three DOS of figure 2 (same symbols). In this last case the respective contributions of MT (open symbols) and hopping (crossed open symbols) to the photoconductivity are shown along with the total photoconductivity (full lines).

increasing density of states (full symbols). This behaviour agrees with what one would expect with a fixed generation rate and an increasing DOS: the higher the DOS the lower the splitting of the quasi-Fermi levels and consequently the photocurrent. When hopping is taken into account, conduction by MT is dominant at high temperature and hopping transport appears at low temperature for the two lowest DOS. However, the MT contribution to the photoconductivity is affected by the hopping process since the photoconductivity values (open symbols) are always below the photoconductivity values obtained with MT alone. For the highest DOS, hopping appears to be the main process of transport over the whole range of temperature, the hopping contribution to the photoconductivity being always larger than the MT contribution. In the following we propose an explanation for these two characteristic behaviours.

In figure 5 there are displayed the evolutions of the variations of the occupation functions with the generation rate at  $T = 310 \text{ K}$  for the lowest density of states of figure 2 when MT is considered alone and when the hopping process is taken into account. In the case of MT alone the evolution is as predicted from the theory developed by Taylor and Simmons for a single species of states [19]. The recombination zone is delimited by the plateau of the occupation function at say  $f = 0.85$  and the energy width of this plateau increases with the generation rates simply because with increasing flux the recombination zone enlarges to reach steady equilibrium. In this case the carriers move from one localized state to the other by emission from the starting state toward the extended states followed by the capture by the other localized state. When hopping is taken into account the variations with energy of the occupation functions are completely different, the hopping resulting in a condensation of carriers in the localized levels around the dark Fermi level position. This is obviously due

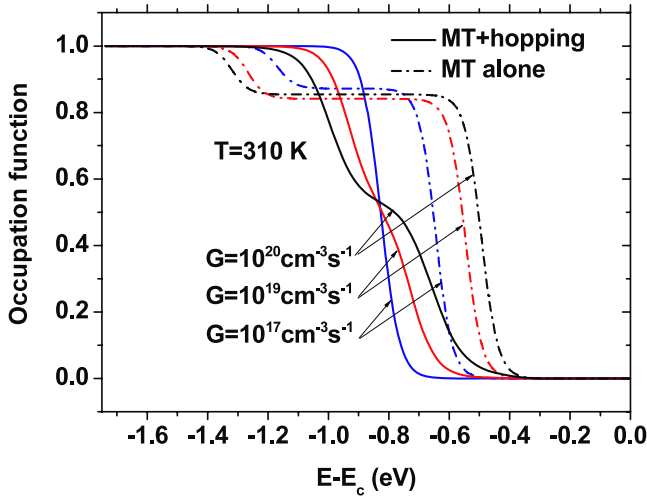


**Figure 5.** Evolution with the generation rate of the variations with energy of the occupation function under illumination at  $T = 310$  K. These curves were calculated considering the MT alone and the MT plus the hopping process, introducing the lowest density of states of figure 2 in the simulation.

to the fact that with a DOS that is not varying too rapidly, electrons can move down by hopping, filling the empty levels. As a consequence, the quasi-Fermi levels are closer to the dark Fermi level position than when only MT is considered and the number of free carriers decreases accordingly. This explains why under steady state illumination, though the photoconductivity is mainly controlled by multiple trapping at high temperatures, the introduction of hopping lowers the photoconductivity values compared to the case in which MT is considered alone (see in figure 4 the open and full triangle curves).

It can be seen in figure 4 that if the DOS is increased by a factor of a hundred, hopping is the dominant conduction process over the whole range of temperature (open squares). The reason for this dominance of hopping is twofold. It could be due to an increase of the hopping carriers and/or an increase of their mobility. The generation rates being the same for all three DOS ( $G = 10^{17} \text{ cm}^{-3} \text{ s}^{-1}$ ) and the occupation function being quite close to the dark occupation function for the lowest DOS (see figure 5), it is certainly also the case for the highest DOS. This latter being a hundred times higher, one may expect to have a hundred times more electrons available for hopping. However, the number of available sites for hopping has also increased with the increase of the DOS and the hopping mobility is probably enhanced. Indeed, if we define  $\bar{\mu}_{\text{hop}} = \frac{q}{6kT} \int_{E_v}^{E_c} \int_{E_v}^{E_c} \Gamma_{E,E'} g(E') [1 - f(E')] r_{E'}^2 dE' dE$  as an average hopping mobility over the gap states, we have calculated that this average mobility increases by a factor of 2.4 from the lowest to the highest DOS at 200 K with a generation rate of  $G = 10^{17} \text{ cm}^{-3} \text{ s}^{-1}$ . Though on average the increase of the mobility is only 2.4, the gain in the hopping photoconductivity that includes a  $g(E)f(E)$  product (see equation (8)) may be more important for some states and it would explain why around 200 K the hopping contribution is multiplied by a factor around 1400 between the lowest and the highest DOS when the DOS ratio is only a factor of a hundred.

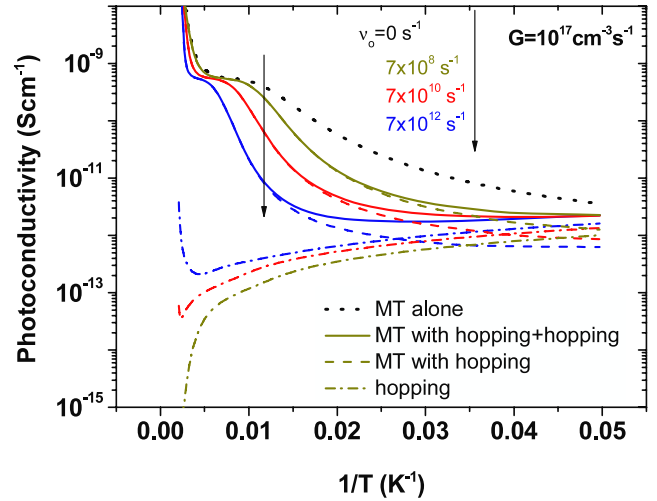


**Figure 6.** Evolution with the attempt-to-hop frequency of the Arrhenius plot of the photoconductivity. The respective contributions of MT (alone or with hopping) and hopping are displayed for comparison along with the sum of the two contributions (MT with hopping + hopping).

The fact that hopping can alter the MT contribution to the photoconductivity even when MT is clearly the dominant process, for instance at high temperature, pushes us to search for a signature of hopping in the dc photoconductivity curves. We display in figure 6 the evolution with the attempt-to-hop frequency of the photoconductivity as function of temperature calculated taking into account the lowest DOS of figure 2. In this figure  $\nu_0$  was taken equal to 0 (MT alone),  $7 \times 10^8$ ,  $7 \times 10^{10}$  and  $7 \times 10^{12} \text{ s}^{-1}$ . As expected, the higher the  $\nu_0$ , the higher the hopping contribution. With increasing  $\nu_0$  it can be also seen that (i) the range of temperature for which MT is the dominant process of photoconductivity is shrinking, (ii) in this range, though MT is the dominant process, the photoconductivity absolute value is decreasing for the same reason as was given above, and (iii) the hopping contribution at low temperature reveals, by the occurrence of a plateau, the photoconductivity turning to being independent of  $T$ , and, in agreement with (i), the higher  $\nu_0$ , the higher the temperature at which the plateau starts. This result agrees with the experimental results reported by Fritzsche [8].

Hence, evidence for hopping can be obtained, in dc photoconductivity, if at low temperature a zone appears for which the photoconductivity values are temperature independent. However, this behaviour corresponds to a very important contribution of hopping, as is the case with a quite high  $\nu_0$  value, and it can be seen that with lower  $\nu_0$  values, hopping definitely has an influence on the photoconductivity values without being revealed by the clear occurrence of a plateau at low temperature. Thus, it can be quite difficult to obtain evidence for hopping with dc measurements. We shall show below that ac measurements are probably more sensitive indicators.

#### 4. Modulated photoconductivity

As mentioned in the introduction, the modulated photocurrent technique was first proposed by Oheda [1] and since then it has been intensively studied and used to investigate the defects of highly resistive semiconductors [20–24]. We must underline that hopping transport was never considered in any of the previous theoretical developments. Actually, this can be easily understood since, considering equations (11) and (12), it seems rather difficult to derive an equation linking the probed density of states to experimental parameters like the modulus and phase shift of the ac photocurrent. In this section, we shall first recall the basics of the theory of modulated photoconductivity when MT is considered alone and further show the expected influence of hopping on the experimental results.

The sample fitted with two parallel ohmic electrodes, say between one to two mm apart, is biased by a dc voltage and illuminated by a flux of light modulated at an angular frequency  $\omega$ . The photon energy is chosen to be slightly higher than the band gap of the semiconductor studied. The ac component of the flux  $F_{ac}$  being considered as a small perturbation of the dc component of the flux  $F_{dc}$  and assuming that one type of carrier is predominant, it was shown that the density of states  $N$  at an energy  $E$  below the extended states interacting with these carriers can be estimated by recording the modulus of the alternating current  $I_{ac}$  resulting from the modulated flux as well as its phase shift  $\phi$  referred to  $F_{ac}$ . Assuming that electrons are the majority carriers, at a given temperature  $T$  one can estimate the quantity  $NC_n/\mu_n$  from experimental parameters by using the relation [2, 4]

$$\frac{NC_n}{\mu_n} = \frac{2}{\pi k_b T} S q G_{ac} \xi \frac{\sin(\phi)}{|I_{ac}|}, \quad (13)$$

where  $\xi$  is the applied electric field,  $G_{ac}$  the alternating generation rate and  $S$  the conduction cross section through which the current is flowing. Another estimate of  $NC_n/\mu_n$  was proposed by Hattori *et al* from the relation [3]

$$\frac{NC_n}{\mu_n} = \frac{S q G_{ac} \xi}{k_b T} \omega \frac{d}{d\omega} \left( \frac{\cos(\phi)}{|I_{ac}|} \right). \quad (14)$$

In both methods the quantity  $NC_n/\mu_n$ , that we shall call the reduced DOS or r-DOS in the following, depends only on experimentally known parameters. Theoretically, equations (13) and (14) have been obtained assuming that the transport is achieved by multiple-trapping events. In this case it was shown that the states probed by the experiments are those for which the emission rates equal the excitation angular frequency  $\omega$ . That is why the energy scaling is achieved following the equation

$$\Delta E = k_b T \ln(\nu/\omega). \quad (15)$$

We have written  $\Delta E$  because it is *a priori* impossible to know from the experiment whether the predominant carriers are holes or electrons. Hence, the probed density of states may be  $\Delta E$  above (below) the valence (conduction) band if holes (electrons) are the main carriers giving rise to the

ac photocurrent. The parameter  $\nu$ , also called the attempt-to-escape frequency, is defined as  $C \times N_{eq}$  in which  $N_{eq}$  is the equivalent density of states at the band edge for the predominant carriers. In the MPC experiment  $\nu$  is the only adjustable parameter. In the present case we are dealing with a-Si:H in which electrons are known to be the majority carriers. Taking account of the data taken to run the simulations we have  $\nu = 5 \times 10^{11} \text{ s}^{-1}$  at 300 K, a value close to the one found experimentally for a-Si:H [16]. It is this value that will be used in the following for the energy scaling in the plots of the MPC spectra coming from the numerical simulations.

According to equation (15) a DOS spectroscopy can be achieved by varying either  $\omega$  at a given temperature or  $T$  at a given  $\omega$ . Actually, experimentally, both are done for  $\omega$  in a logarithm; it is almost impossible to cover a very large energy range by just varying this parameter. Experimentally, at a given temperature, the frequencies  $fr$  of the modulation were varied from 12 Hz to 40 kHz in steps such that  $fr_{i+1} = fr_i \times 1.5$  and the investigation was for the same range of frequencies in our numerical simulations. According to equation (15), the higher the frequency, or the lower the temperature, the closer to the band the deduced density of states, from equations (13) or (14).

Since equations (13) and (14) are the only ones at our disposal for performing DOS spectroscopy it is these equations that can be used to try to perform DOS spectroscopy from experimental or simulated results even in the case where hopping presents a non-negligible contribution. We display in figure 7 the DOS spectroscopies calculated using equation (13) applied to the results of numerical simulations in which the different DOS of figure 2 have been taken into account. Calculations were achieved either assuming MT alone or MT plus a hopping contribution with a  $\nu_0 = 7 \times 10^{12} \text{ s}^{-1}$ . The following parameters were assumed: a dc generation rate  $G_{dc} = 10^{17} \text{ cm}^{-3} \text{ s}^{-1}$ , an ac generation rate  $G_{ac} = G_{dc}/10$  as for all the numerical simulations of the MPC experiment, a conduction cross section  $S = 2.25 \times 10^{-5} \text{ cm}^2$  and a dc electric field  $\xi = 3000 \text{ V cm}^{-1}$ .

Clearly, when MT is considered alone, the DOS introduced are well reproduced since all the curves obtained from equation (13) at different temperatures (full lines) are superimposing and follow quite accurately the chosen DOS (dashed line). With the introduction of hopping (dotted lines) the DOS are no longer reproduced by means of equation (13). For the lowest DOS only the points derived at high frequency are close to the introduced DOS. For the two others and higher DOSs the treatment of the modulated photocurrent data does not lead to any reconstruction of the DOS. In addition, the higher the DOS, the poorer the reconstruction. This is not surprising since we have show that in dc measurements the hopping process was more and more dominant with increasing DOS (see figure 4), and we are faced with the same increasing influence in ac measurements.

A tentative explanation is the following. It can be seen in equation (13) that the quantity  $NC_n/\mu_n$  is proportional to the reciprocal of the modulus of the alternating current. To derive this quantity, the alternating current is assumed to reflect the movement of carriers in the extended states since only MT

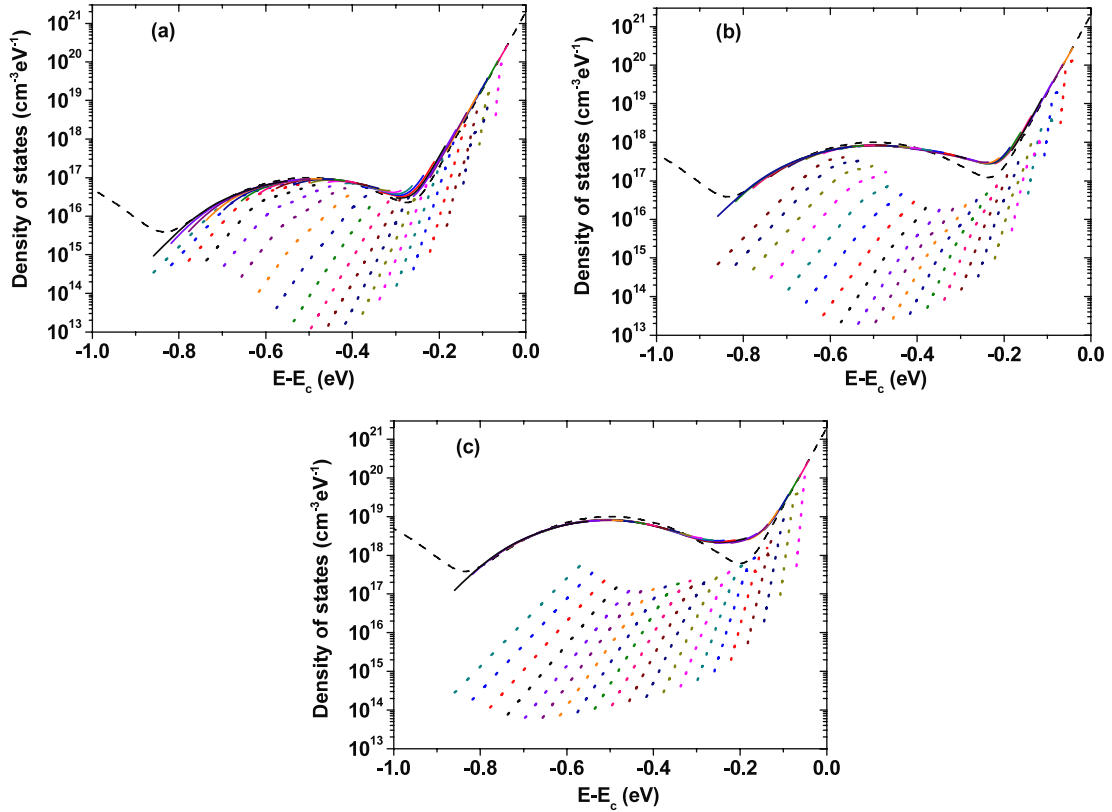


**Figure 7.** Reconstruction of the DOS from equation (13) taking account of the MT alone (full lines) and of MT plus hopping (dotted lines) for the three DOS of figure 2 (dashed lines) from the lowest in (a) to the highest in (c). The values of  $C_n$  and  $\mu_n$  were taken equal to those introduced in the simulation used to obtain the MPC DOS values from the MPC r-DOS. Temperature was varied from 440 K to 40 K in 20 K steps.

has been considered. If a hopping component adds to the total alternating current, its modulus  $|I_{ac}|$  increases and this is reflected in a decrease of the deduced DOS. Besides, the numerical simulation has shown that the hopping contribution to  $|I_{ac}|$  was increasing with decreasing frequency. A possible explanation is that at low frequencies more carriers participate in hopping as they have more ‘time’ to find a hopping site than at high frequency. The final results are these ‘segments’ or ‘tails’, plotted for each temperature, almost parallel to one another when the DOS is high, the deeper part being obtained at low  $\omega$  and the part closer to the band corresponding to high  $\omega$ .

These ‘segments’ resemble a lot what one would calculate if the MPC experiment was performed or simulated with a rather high dc flux. The influence of the dc flux on the final DOS reconstruction is shown in figures 8(a) and (b). For these two figure parts the numerical calculation was achieved assuming MT alone. It can be seen that whereas in figure 8(a) the introduced DOS is rather well reproduced with  $G_{dc} = 10^{17} \text{ cm}^{-3} \text{ s}^{-1}$ , in figure 8(b) only the points obtained at high frequencies follow the DOS ( $G_{dc} = 10^{20} \text{ cm}^{-3} \text{ s}^{-1}$ ). An explanation of this behaviour was already provided [4] and it was also demonstrated experimentally [25]. Basically, the MPC signal is sensitive to the empty states. If the dc flux is low, even the deepest states probed at low frequency are empty. If the dc flux is too high, the splitting of the quasi-Fermi levels increases and the states probed at low frequency

are partly filled and the density of empty states decreases. At these low frequencies the MPC signal behaves as if the DOS was lower than the true DOS, which is precisely the case for the density of *empty* states, and the final result after treatment with equation (13) is a calculated DOS lower than the real one.

In figures 8(c) and (d) the MPC was simulated introducing the same DOS as for figures 8(a) and (b) but taking account of a hopping contribution assuming  $\nu_0 = 7 \times 10^{12} \text{ s}^{-1}$ . It can be seen that the flux influence is less visible since the same ‘tails’ appear at each temperature even at low generation rate. Clearly hopping induces behaviour of the MPC treatment as if the dc flux was too high but, in contrast to what can be achieved if MT is the only process of transport, adjustment of the dc flux has only little influence on the final results. Let us recall that the ac generation rate was taken as  $G_{ac} = G_{dc}/10$ . The weak dependence on the flux of the MPC curves probably comes from the fact that the hopping contribution to the ac current is linked to the number of trapped carriers responding to the excitation, a number depending almost linearly on  $G_{ac}$  if the trapping states are not saturated by the dc component of the flux. If the hopping process is predominant, then the ratio  $G_{ac}/|I_{ac}|$  in equation (13) is only slightly dependent on the generation rates and the DOS deduced from this equation does not evolve much with the generation rate.

One can therefore take advantage of this property to easily obtain evidence of the occurrence or absence of the hopping

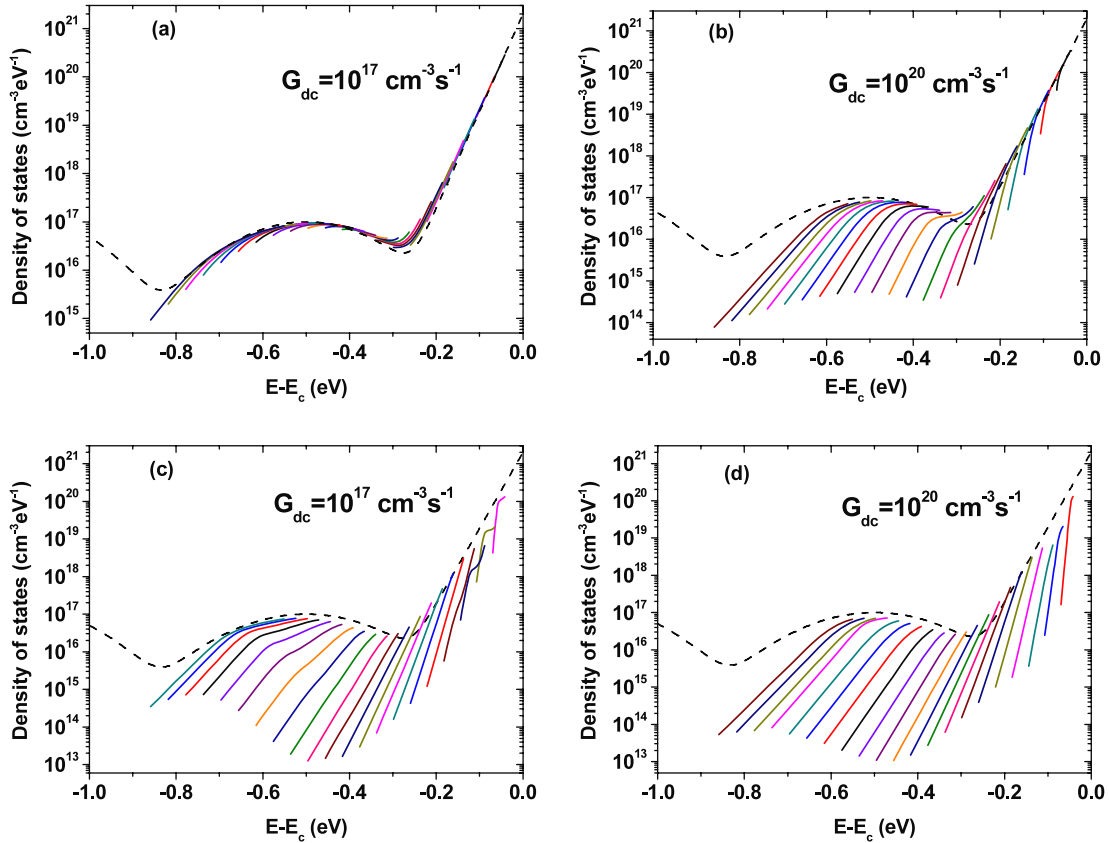


**Figure 8.** DOS reconstruction from numerical calculations performed on the lowest DOS of figure 2 (dashed line) using equation (13) and the  $C_n$  and  $\mu_n$  values of the simulation. In (a) and (b) MT alone was considered with  $G_{dc} = 10^{17} \text{ cm}^{-3} \text{ s}^{-1}$  in (a) and  $G_{dc} = 10^{20} \text{ cm}^{-3} \text{ s}^{-1}$  in (b). In (c) and (d) hopping was taken into account with  $\nu_0 = 7 \times 10^{12} \text{ s}^{-1}$  and with  $G_{dc} = 10^{17} \text{ cm}^{-3} \text{ s}^{-1}$  in (c) and  $G_{dc} = 10^{20} \text{ cm}^{-3} \text{ s}^{-1}$  in (d).

process in the global transport of carriers. We shall show in the next section that it can be experimentally used in the case of hydrogenated amorphous silicon.

However, before presenting experimental results we want to stress the influence of  $\nu_0$  on the DOS reconstruction from MPC data.

In figure 9 are displayed the DOS reconstructed from the results of a MPC simulation taking account the lowest DOS of figure 2. It can be seen that, as expected, as  $\nu_0$  decreases the agreement between the introduced DOS and the calculated MPC DOS improves at least at high temperatures. However, even with a very low value of  $\nu_0$  ( $7 \times 10^8 \text{ s}^{-1}$ ) the hopping contribution can be observed at low temperature. This hopping contribution appears clearly at the two lowest temperatures (upper right corner of figure 9(c)) for which the MPC DOS reconstructed from equation (13) departs from the introduced DOS especially at low frequencies (i.e. at deeper energies). Such a behaviour cannot be seen when MT is taken alone (see for instance figure 8(a)). Again it can also be seen that the flux variations have little influence on the MPC DOS curves when hopping contribution is significant. Indeed, a comparison of figures 9(c) and (d) shows that a clear evolution of the reconstructed DOS can be observed if the generation rate is increased at least for the deepest states. For the shallowest states of the band tail, states for which the hopping contribution is high, the modification of the two curves obtained at low temperatures, if any, is hardly visible.

## 5. Experimental results

Experiments were performed on a standard a-Si:H thin film deposited on glass at low power (5 mW) and low pressure (5 mTorr) by means of a radio frequency (13.56 MHz) powered plasma enhanced chemical vapour deposition (rf-PECVD) system. The deposition temperature was 200 °C. Two parallel aluminium ohmic contacts (1 cm long and 2 mm apart) were deposited on top of the film. The sample was set onto the cold finger of a helium closed-cycle cryostat operating in the temperature range 10–310 K. The experiments, with dc photoconductivity and modulated photoconductivity, were achieved with a wavelength of 650 nm and dc fluxes in the range  $10^{14}$ – $10^{15} \text{ cm}^{-2} \text{ s}^{-1}$ . For the modulated photoconductivity experiment the ac flux was four times lower than the dc flux. As already mentioned, the frequencies of the modulation were in the range 12 Hz–40 kHz and chosen such that  $fr_{i+1} = 1.5 \times fr_i$ .

In figure 10 there is displayed the evolution of the dc photoconductivity with temperature varying in the range 18–300 K. The light flux was  $F_{dc} = 10^{14} \text{ cm}^{-2} \text{ s}^{-1}$ . The observed behaviour is rather typical: from high temperature the photocurrent decreases and a kink appears around 100 K, that for some samples is more pronounced and even gives rise to a quenching of the photoconductivity. Further, the curve still decreases with decreasing  $T$  until it flattens around 25 K. This evolution may be interpreted as it was by Fritzsche *et al* [8].

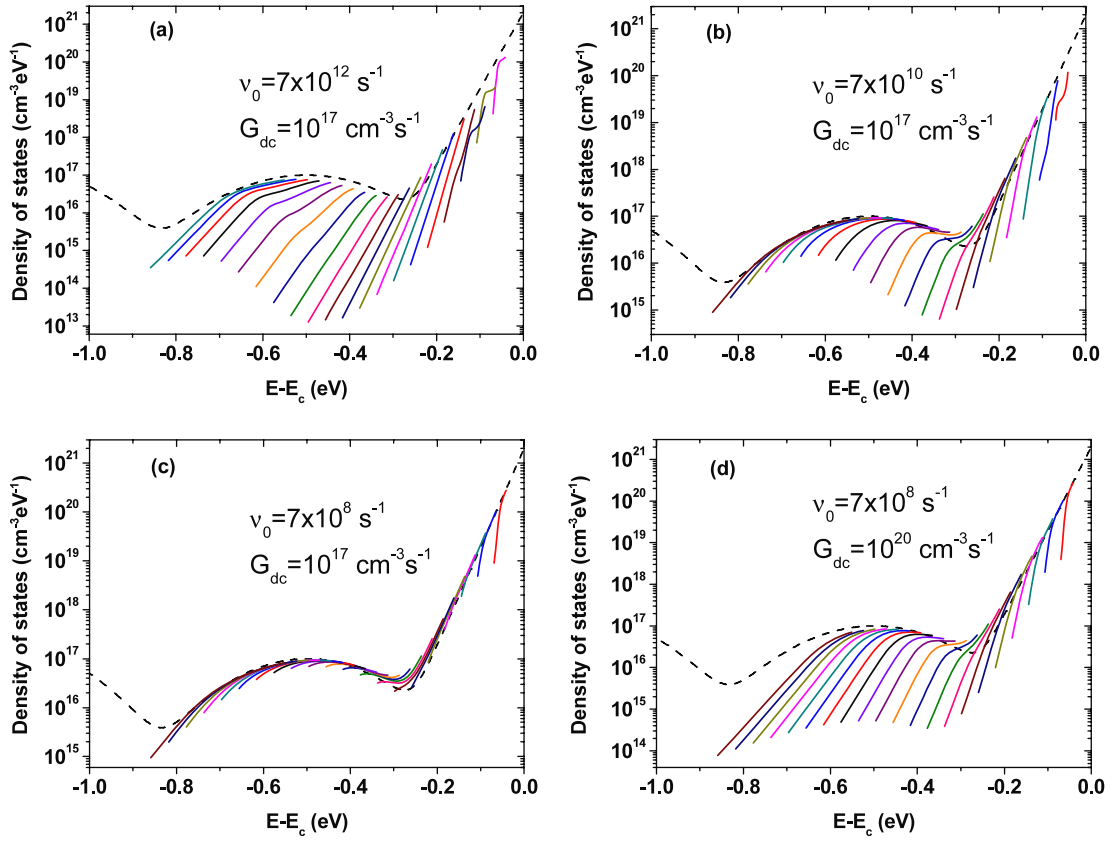


**Figure 9.** Influence of the  $\nu_0$  values on the DOS reconstruction. The DOS introduced in the simulation (dashed line) was the lowest of figure 2. In (a), (b) and (c) the generation remains the same:  $G_{dc} = 10^{17} \text{ cm}^{-3} \text{ s}^{-1}$  with  $\nu_0 = 7 \times 10^{12} \text{ s}^{-1}$ ,  $7 \times 10^{10} \text{ s}^{-1}$  and  $7 \times 10^8 \text{ s}^{-1}$  respectively. In (d)  $G_{dc} = 10^{20} \text{ cm}^{-3} \text{ s}^{-1}$  with  $\nu_0 = 7 \times 10^8 \text{ s}^{-1}$ .

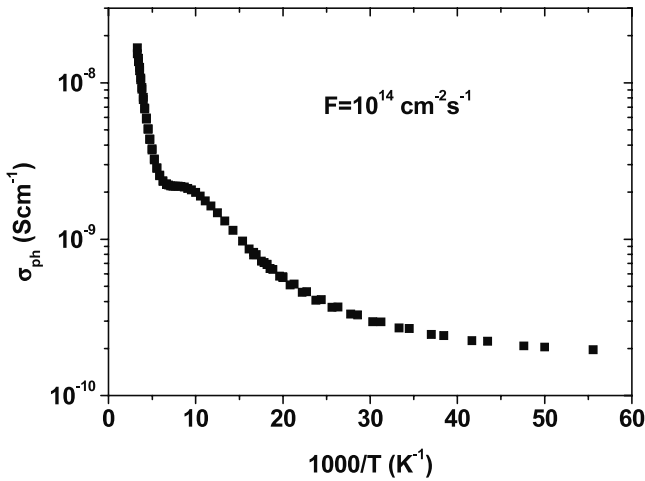


**Figure 10.** Photoconductivity measured for a standard a-Si:H film with a flux of  $10^{14} \text{ cm}^{-2} \text{ s}^{-1}$  in the temperature range 18–300 K.

However, we do not observe a clear plateau at low temperatures where hopping is probably the dominant process and it is rather difficult to determine clearly the temperature at which hopping begins to dominate over multiple trapping.

We have also performed modulated photoconductivity measurements. The investigations were essentially done at low temperature, each 10 K from 150 to 40 K. The results are

displayed in figure 11. Two fluxes were used: a dc flux of  $10^{15} \text{ cm}^{-2} \text{ s}^{-1}$  ( $F_{ac} = 2.5 \times 10^{14} \text{ cm}^{-2} \text{ s}^{-1}$ , full lines), and a dc flux of  $2 \times 10^{14} \text{ cm}^{-2} \text{ s}^{-1}$  ( $F_{ac} = 5 \times 10^{13} \text{ cm}^{-2} \text{ s}^{-1}$ , open symbols). It can be seen that the reconstructed r-DOS consists mainly of straight line segments, almost parallel, as is the case when hopping dominates the transport according to the previous theoretical developments. It can be also seen that for 100 K and temperatures below there is no influence of the flux used on the calculated r-DOS, the symbols perfectly superimposing on the full lines, again as expected from the model when hopping dominates the transport. At 150 K and at the lowest frequency we find an increase by a factor of 2 on the calculated r-DOS when the flux is decreased by a factor of 5 showing that MT still influences the transport process. To test the possible occurrence of hopping at higher temperature we have performed a measurement at 250 K. At low frequency the modulated photoconductivity results lead to an increase by a factor of 5 of the calculated r-DOS showing that the hopping contribution is certainly very small.

Despite the clear influence of hopping in the results for modulated photoconductivity at low temperature, we have estimated the slope of the conduction band tail by taking the upper envelope of the curves and obtained an order of magnitude of its characteristic temperature  $T_c = 280 \text{ K}$  close to the one expected from the literature (see for instance [26] and references therein).

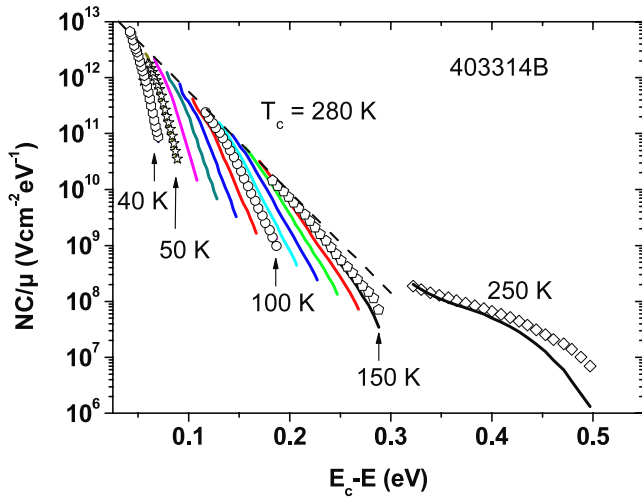


**Figure 11.** Reconstructed r-DOS, from the results of the modulated photoconductivity experiment performed at different temperatures on an a-Si:H film. A dc flux of  $10^{15} \text{ cm}^{-2} \text{ s}^{-1}$  results in the full lines whereas a dc flux of  $2 \times 10^{14} \text{ cm}^{-2} \text{ s}^{-1}$  results in the open symbol reconstruction. A dashed line has been added to underline the conduction band tail slope giving an order of magnitude of the band tail characteristic temperature  $T_c$ .

We can provide a tentative explanation for why hopping is dominating over multiple trapping in the modulated photoconductivity experiment performed at low temperatures. The theoretical treatment of the MPC being based only on multiple trapping, it can be demonstrated under this hypothesis that the probed states (i.e. those with the greatest relative influence on the ac response phase shift) are those located around an energy  $E_\omega$  for which the rate of emission toward the extended states equals the angular frequency  $\omega$  of the light modulation. The states located closer to the band are emitting carriers too rapidly to introduce a delay, i.e. a phase shift, in the ac response of the material to the excitation. The states located deeper do not introduce a phase shift either because the delay of emission is too long to play a role in the ac response of the material. This also means that the traps located deeper than  $E_\omega$  are filled with carriers that can be considered as ‘frozen in’ as far as MT is concerned, and the number of these ‘frozen in’ carriers increases with decreasing temperature as  $E_\omega$  approaches the band edge since it parallels the band tail state distribution. However, these carriers are certainly not ‘frozen in’ as far as hopping is concerned and since the number of carriers and the number of available states increase while  $E_\omega$  approaches the band edge with decreasing temperature, their hopping contribution becomes more and more important. Besides, at low frequency the number of hops is probably higher in a period of modulation than at high frequency. The consequence is a modulus of the ac current that is higher than it would be if MT was the only process involved, and even higher if the frequency of the modulation is low, and it results in a lower  $NC/\mu$  value according to equation (13).

The dependence on the generation rate is also slight because, unless the states below  $E_\omega$  are saturated, the contribution to the hopping is nearly proportional to the number of carriers trapped deeper than  $E_\omega$ , which is proportional to

$G_{ac}$ . Therefore, the ratio  $G_{ac}/|I_{ac}|$  stays nearly constant in equation (13) as soon as hopping becomes predominant.

In conclusion, the hopping contribution depends not only on the hopping process itself, but also on the experiment performed to obtain evidence for it, because it is clear that at 100 K in dc the hopping contribution is very small—at least it would be very difficult to find evidence for it—whereas it appears to be quite predominant in ac measurements achieved at the same temperature (see figures 10 and 11).

This last remark indicates in which direction future work has to be extended. Indeed, it was shown in previous publications that by combining different experiments (e.g. MPC at low frequency or standard photoconductivity) based on the photoconductive properties of the material studied, it was possible to extract several transport parameters [16]. By applying these techniques to a-Si:H, it was shown that not only the DOS shape but also orders of magnitude of the conduction and valence band tail capture coefficients, as well as of the free electron mobility, could be derived. It is the  $C_n$  value coming from these recent results that we have used to scale the energy axis of figure 11 from equation (15) taking  $C_n = 4 \times 10^{-8} \text{ cm}^3 \text{ s}^{-1}$  and  $N_c = 2.5 \times 10^{19} \text{ cm}^{-3}$  at 300 K to obtain  $\nu = C_n N_c = 10^{12} \text{ s}^{-1}$ . The reader may note that taking  $C_n$  in the range of  $10^{-8}$ – $10^{-7} \text{ cm}^3 \text{ s}^{-1}$  would have led to  $T_c$  in the range 254–300 K. However, the major problem that we are faced with is not the uncertainty that we have concerning the  $T_c$  value, here around  $\pm 10\%$ , but that all the developments up to now for all the photoconductivity results obtained from 100 K and above were considering only the multiple-trapping approach and were completely neglecting the hopping influence. Our theoretical and experimental results show that it is certainly not possible to neglect systematically the hopping contribution. Future work would at least include checking the influence of hopping on the conclusions drawn from experiments whose theoretical analysis only considered multiple-trapping processes. One may think for instance about the physical meanings of the well known  $\gamma$  coefficient relating photoconductivity and dc flux ( $\sigma \approx F^\gamma$ ). The reader may note that this idea of reconsidering the results of ‘classical’ experiments taking the hopping contribution into account is not original, since it was already proposed by Main *et al* for the interpretation of transient photoconductivity [13]; but it can be foreseen as essential to a better understanding of the transport mechanisms in disordered materials.

The last point that we can address is giving an estimate of  $\nu_0$  for our a-Si:H sample. Considering the lowest DOS of figure 2 a rapid calculation gives a maximum  $NC/\mu$  value equal to  $10^8 \text{ V cm}^{-2} \text{ eV}^{-1}$ , approximately the value that we obtain experimentally from the measurements performed at 250 K. Considering the simulation results of figure 9 it is clear that a value of  $7 \times 10^{12} \text{ s}^{-1}$  is substantially too high, whereas the lowest value that we used ( $7 \times 10^8 \text{ s}^{-1}$ ) appears to be slightly too low. We may suggest an order of magnitude of  $5 \times 10^9 \text{ s}^{-1}$  as a good approximation for the attempt-to-hop frequency in a-Si:H.

## 6. Conclusion

On the basis of the analytical procedure for hopping proposed by Marshall we have developed equations for modelling the

transport of carriers both under steady state and modulated illuminations taking into account the hopping and the multiple-trapping processes. Like Marshall, we have attempted to introduce the gap state occupancy in the hopping probability. A numerical simulation has been developed using these equations and we have studied in a first step the influence of some parameters, such as the DOS and the attempt-to-hop frequency, on the steady state photoconductivity. We have shown that even when MT is likely to be the main transport process (e.g. at high temperature), hopping clearly has an influence, in comparison with situations in which MT is considered to be the only transport process. Of course, the hopping influence depends on the attempt-to-hop frequency, but our simulation shows that this influence is still present even when  $\nu_0$  is as low as  $5 \times 10^8 \text{ s}^{-1}$  though it can hardly be detected from steady state measurements. In a second step we have investigated the influence of hopping on the modulated photoconductivity data. We have shown that it was not possible to derive a simple expression for the DOS reconstruction as was the case when only MT was considered. Therefore we have used the only equations at our disposal and have shown that the hopping process influence leads to a DOS reconstruction that can be far from the true DOS. In the case of a significant influence of hopping, the reconstructed DOS behaves as if the dc flux was too important, as revealed by the ‘tails’ obtained at the different temperatures of the measurements. However, in the case of the hopping influence on the MPC data, and contrary to what is expected when the dc flux is chosen too high, the data seem to be less sensitive, or even completely insensitive, to the variations of the flux of light. This property was used to provide evidence of the hopping influence on the transport processes in an a-Si:H film. From steady state photoconductivity measurements one would deduce that hopping has a predominant influence below 30 K, whereas modulated photoconductivity experimental results demonstrate that hopping influences the transport processes for temperature as high as 100 K. The comparison of MPC experimental and simulated results allows us to propose an order of magnitude of the attempt-to-hop frequency of  $5 \times 10^9 \text{ s}^{-1}$  in a-Si:H. Finally, all these results suggest that a reviewed analysis of some classical experiments has to be performed to improve our insight into transport mechanisms in disordered solids.

### Acknowledgments

S Tobbeche thanks the Algerian Ministry of Higher Education and Research for support and a grant to visit Laboratoire de Génie Electrique de Paris.

### References

- [1] Oheda H 1981 *J. Appl. Phys.* **52** 6693
- [2] Brüggemann R, Main C, Berkin J and Reynolds S 1990 *Phil. Mag. B* **62** 29
- [3] Hattori K, Niwano Y, Okamoto H and Hamakawa Y 1991 *J. Non-Cryst. Solids* **137/138** 363
- [4] Longeaud C and Kleider J P 1992 *Phys. Rev. B* **45** 11672
- [5] Cloude C, Spear W E, Lecomber P G and Hourd A C 1986 *Phil. Mag. B* **54** L113
- [6] Spear W E and Cloude S C 1988 *Phil. Mag. B* **58** 467
- [7] Johanson R E 1992 *Phys. Rev. B* **45** 4089
- [8] Fritzsche H, Yoon B-G, Chi D-Z and Tran M Q 1985 *J. Non-Cryst. Solids* **141** 123
- [9] Monroe D 1985 *Phys. Rev. Lett.* **54** 146
- [10] Shklovskii B I, Levin E I, Fritzsche H and Baranovskii S D 1990 *Advances in Disordered Semiconductors* vol 3, ed H Fritzsche (Singapore: World Scientific) p 161
- [11] Merazga A, Tobbeche S, Main C, Al-Shashrani A and Reynolds S 2006 *J. Phys.: Condens. Matter* **18** 3721
- [12] Marshall J M 2000 *Phil. Mag. Lett.* **80** 691
- [13] Main C, Marshall J M and Reynolds S 2005 *J. Optoelectron. Adv. Mater.* **7** 107
- [14] Tobbeche S and Merazga A 2007 *J. Phys.: Condens. Matter* **19** 436220
- [15] Biran A, Breiner M and Larousse N 2004 *MATLAB pour l'ingénieur, Version 6 et 7* Pearson Education Ed. (France)
- [16] Longeaud C, Schmidt J A and Koropeccki R R 2006 *Phys. Rev. B* **73** 235317
- [17] Mott N F and Davis E A 1979 *Electronic Processes in Non-Crystalline Materials* ed W Marshall and D H Wilkinson (Oxford: Oxford University Press)
- [18] Marshall J and Main C 2008 *J. Phys.: Condens. Matter* **20** 285210
- [19] Taylor G W and Simmons J G 1972 *J. Non-Cryst. Solids* **8–10** 940
- [20] Longeaud C, Kleider J P, Kaminski P, Koslowski R, Pawlowski M and Cwirko J 1999 *Semicond. Sci. Technol.* **14** 747
- [21] Verstraeten D, Longeaud C, Ben Mahmoud A, von Bardeleben H J, Launay J C, Viraphong O and Lemaire Ph C 2003 *Semicond. Sci. Technol.* **18** 919
- [22] Frejlich J, Montenegro R, Inocente N R Jr, Dos Santos P V, Launay J C, Longeaud C and Carvalho J F 2007 *J. Appl. Phys.* **101** 043101
- [23] Cohen J D and Kwon D 1998 *J. Non-Cryst. Solids* **227** 348
- [24] Kounavis P and Mytilineou E 1999 *J. Phys.: Condens. Matter* **11** 9105
- [25] Kleider J P, Longeaud C and Glodt O 1991 *J. Non-Cryst. Solids* **137/138** 447
- [26] Tiedje T 1984 *Semiconductors and Semimetals* vol 21C, ed J Pankove (New York: Academic) pp 207–38